Enrichment of C-14 on Surface Deposits of Oldbury Reactor Graphite Investigated with the Use of Magnetic Sector Secondary Ion Mass Spectrometry – 15076

Liam Payne *, Peter J. Heard *, Thomas B. Scott *

* Interface Analysis Centre, School of Physics, University of Bristol

ABSTRACT

Large quantities of irradiated graphite containing C-14 will arise from the decommissioning of the UK's Magnox power stations. Magnetic sector secondary ion mass spectrometry (MS-SIMS) has been used to investigate the distribution of this radioisotope within a number of trepanned graphite samples from a variety of radial and axial positions within reactor one at Oldbury, a Magnox nuclear reactor. The methodology used for these determinations ensured that possible mass interferences between C-14 species and oxygen-bearing species were eliminated from the analysis. This work indicates that a carbonaceous deposit found on exposed channel wall face samples has a relative C-14 enrichment compared to the underlying graphite, with concentrations calculated between approximately 5 and 55 ppm. Samples without this deposit gave C-14 concentrations below the limits of detection of the instrument, verifying that the enrichment is due to the deposit. Variations in C-14 concentration with sample height have been shown, with samples lower in the core having an increased C-14 concentration compared with those higher up.

INTRODUCTION

Background

The low capture and high scattering cross-sections of graphite has led to the use of this material as a moderator and reflector material in gas-cooled nuclear reactors [1, 2]. During operational lifetime fast neutron bombardment results in the formation of several activation products [3] and therefore disposal of graphite requires a suitable radioactive waste management strategy [1, 4]. The decommissioning of the first generation of gas-cooled, graphite-moderated (Magnox) reactors in the United Kingdom will lead to approximately 45,000 m^3 of irradiated graphite waste requiring disposal to a geological disposal facility (GDF) in the UK [5]. The graphite contains a major proportion of the carbon-14 in the UK inventory. Carbon-14 is a significant radionuclide for safety assessments of a GDF in the UK [6] because it has a sufficiently long half-life (5730 years), allied with the potential for formation of gaseous species, for its release to be of relevance after closure of a GDF [7].

Carbon-14 Formation in Graphite

Neutron bombardment of graphite leads to the production of C-14, primarily through neutron capture by the incorporated species N-14, C-13 and O-17 [8], Equations 1-3 respectively. Due to the low isotopic abundance and low cross section of O-17, Table I, graphite from Magnox reactors is unlikely to contain any significant concentrations of C-14 arising from O-17 [8]. C-13 is intrinsically present within the graphite material, and therefore it is more likely that C-14 arising from this will be homogenously distributed throughout the graphite [9]. Throughout the manufacture, assembly and storage of nuclear graphite, air naturally adsorbs onto the surface, introducing nitrogen impurities [9] of up to 10ppm [10].

Additionally air ingress during depressurisation as a result of shutdowns will increase nitrogen availability. Consequently, C-14 arising from N-14 is likely to be inhomogeneously distributed on the surface of the graphite, which includes not only the outer geometrical surface but surfaces present in the extensive, complex pore structure [11]. It has been estimated that over 60% of C-14 produced in moderator graphite is from N-14 with the remainder from C-13 [8].

$$N - 14 + n \rightarrow C - 14 + p \qquad \text{(Eq. 1)}$$

$$C - 13 + n \rightarrow C - 14 + \gamma \qquad \text{(Eq. 2)}$$

$$O - 17 + n \rightarrow C - 14 + \alpha \qquad \text{(Eq. 3)}$$

TABLE I. Carbon-14 precursor properties [9].

Precursor species	Capture cross section (barn)	Isotopic abundance (%)
N-14	1.82	99.6
C-13	0.9×10^{-3}	1.1
O-17	0.24	0.037

Surface Deposits on Irradiated Graphite

Recent research [12] providing post mortem analysis of irradiated graphite from two Magnox reactor cores has highlighted the presence of a non-graphitic, carbonaceous deposit on the exposed surfaces of the graphite bricks (channel and interstitial walls) from one of the reactors that has a pronounced and markedly different morphology to the bulk graphite. Such deposits are of interest in geological disposal of radioactive waste from the decommissioning of Magnox reactors as the deposited material is considered to be transiently present in the reactor during power generation lifetime and is anticipated to contain C-14. Additional research [13] on graphite from Oldbury reactor two has highlighted that there appears to be a readily-releasable fraction of C-14 along with a slowly releasable fraction and a fixed fraction unavailable for release.

During operation of the Oldbury reactor small amounts of carbon monoxide and organic material (methane) were added to the CO_2 coolant to inhibit radiolytic corrosion. The radiolytic polymerisation of these gases generate species that deposit to form a sacrificial layer [14]. Additionally, due to the temperature gradient in Magnox reactors the deposit is believed to be more prevalent in the lower regions of the reactor core due to the lower temperature being more favourable for retention of this deposit [14]. As this non-graphitic carbon deposit is significantly more chemically reactive to air than the underlying graphite [14, 15] there is a possibility that if C-14 is present in this coating it may make up a significant proportion of the readily-releasable fraction described previously.

This work investigates the use of magnetic sector-secondary ion mass spectrometry (MS-SIMS) to determine the concentration of C-14 in irradiated graphite samples trepanned from reactor one at Oldbury Magnox power station in 2004, after 37 years of operation.

EXPERIMENTAL METHOD

Sample Provenance and Preparation

A total of 49 irradiated Pile Grade A (PGA) graphite samples trepanned from the core of Reactor One of Oldbury power station were examined. These samples were not specifically trepanned for this work but were previously examined and subsequently archived by the National Nuclear Laboratory (NNL). Originally a cylindrical trepan of approximately 20mm length was cut into 3 slices by NNL giving a possible total of six sample surfaces to be analysed per trepan set, front and reverse of each slice. The sample set contains fourteen full sets (n=42), two sets with only the front two slices (n=4) and three individual samples (n=3). Full details of the samples are presented in Table II and a scale diagram of sample heights is shown in Figure 1. No further preparation was performed before analysis. Virgin (PGA) graphite material which was surplus from the commissioning of Wylfa power station was provided by Magnox Ltd. to act as a comparator. This material was machined using a diamond cutting wheel, South Bay Technology Inc. Model 650, with deionised water as coolant to give specimens of matching dimensions to the trepanned irradiated samples. All samples were analysed in custom made leaded-brass analysis stubs which supported the samples without the use of adhesives, while offering some radiation shielding.

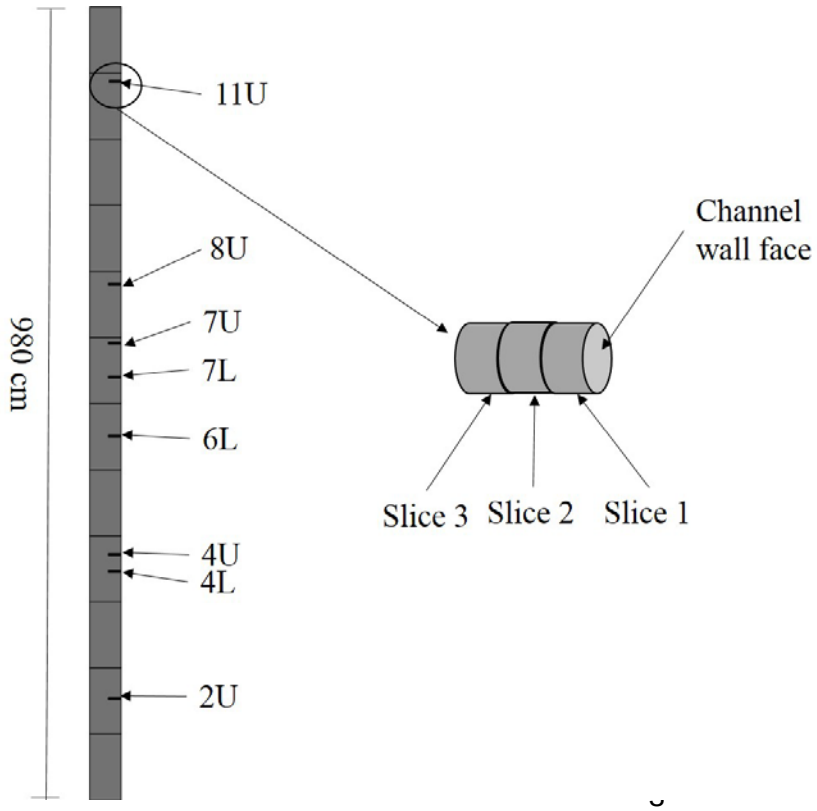

Figure 1: Scale schematic showing sample heights within reactor.

TABLE II. Irradiated graphite sample details.

Channel	Brick	Height (m)	Slice(s)	Fuel/ Interstitial
L13B2	7L	5	1,2,3	Fuel
L13B2	4L	2.7	1,2,3	Fuel
M10	7L	5	1,2,3	Interstitial
M10	4L	2.7	1,2,3	Interstitial
N15A4	8U	6.1	1,2,3	Fuel
N15A4	4U	2.9	1,2,3	Fuel
J15B5	7L	5	1,2,3	Fuel
J15B5	4L	2.7	1,2,3	Fuel
E19B5	8U	6.1	1,2,3	Fuel
E19B5	4U	3	1,2,3	Fuel
F16	7L	5	1,2,3	Interstitial
F16	4L	2.7	1,2,3	Interstitial
J01A4	7U	5.4	1,2,3	Fuel
J01A4	4U	3	1,2,3	Fuel
Q15C5	11U	8.5	1	Fuel
Q15C5	7L	5.1	1	Fuel
Q15C5	6L	4.3	1,2	Fuel
Q15C5	4L	2.7	2	Fuel
Q15C5	2U	1.2	1,2	Fuel

Analytical Methods

Scanning Electron Microscopy

A Helios NanoLab 600i combined SEM/FIB system (FEI, Oregon USA) was used to obtain scanning electron micrographs. Electron micrographs were acquired using an accelerating voltage of 15kV, an electron beam current of 0.17nA and a dwell time of 100µs.

Magnetic Sector-Secondary Ion Mass Spectrometry

Graphite samples were characterised using an in-house built magnetic sector-secondary ion mass spectrometer. Full details of the system are described elsewhere [16]. In summary the system comprised of a focused gallium ion gun (FEI electronically variable aperture type) fitted to a Vacuum Generators model 7035 double-focusing magnetic sector mass analyser with a channeltron ion detector. The system is equipped with an Everhart-Thornley electron detector so that secondary electron images of the sample can be obtained. The equipment was controlled using PISCES software, written in-house by Dayta Systems Ltd (Thornbury, UK).

All analyses were performed in negative ion mode with a gallium ion beam current of 3nA and an ion energy of 25 keV. The sample potential was held at approximately -4 kV.

Survey spectra

Survey spectra from each sample face were acquired by scanning the ion beam over an area of 400µm x 300µm and scanning a mass range of 0-100 Da at 0.05 Da steps with a dwell time of 100 ms per step. The data were used for initial peak identification and instrument calibration.

Depth profiles

Depth profiles were acquired from six equal sized areas of each sample face, choosing sites that generated sufficient secondary ion emission for analysis. These were acquired by scanning the ion beam over an area of 65µm x 55µm and detecting secondary ions over a gated area of approximately 20µm x 15µm. Profiles were collected for 1800 seconds, with the average signal intensity calculated between 200-1800 seconds and subsequently used in the calculation of normalised signal ratios. The Stopping and Range of Ions in Matter (SRIM) [17] was used to estimate the total sputter depth as approximately 300 nm, therefore it is believed that data collected is from the deposit and not underlying graphite as previous work has shown the deposits to be of the order of 5-10 µm thick [12]. Data from the first 200 seconds was discarded, as surface contamination layers were removed. Signals from five mass peaks were recorded during analysis, at mass-to-charge (m/z) values of 16, 24, 26, 27.6 and 28. These correspond to atomic oxygen, carbon-12, diatomic carbon-nitrogen, background and carbon-14 respectively. The di-atomic species were chosen to reduce interferences and because of their high signal strength. Two normalised signal ratios, Equation 4, were calculated; 28/24 for comparison of carbon-14 to carbon-12, and 16/24 to investigate the presence of oxygen so that any CO^- interference at m/z 28 could subsequently be corrected for. A methodology for calculating C-14 concentration involving the exclusion of CO^- interference has been previously described [18] and has been used in this work.

$$r = \frac{S_1 - B}{S_2 - B} \qquad \text{(Eq. 4)}$$

Where: r is the normalised signal, S_1 is the signal of the secondary ion species of interest, S_2 is the signal arising from carbon-12 and B is the background signal.

In summary investigation into possible CO^- interference at m/z = 28 was performed by collecting similar depth profiles from virgin PGA graphite. The graphite was incrementally exposed to research grade oxygen (Cryogenic Rare Gases) during analysis in order to deliberately generate CO^- species on the sample surface. The results allowed a measurement of the normalised 28/24 ratio that will arise from CO^- species alone, enabling CO^- contributions to the m/z =28 peak to be corrected for in subsequent experiments on irradiated samples.

RESULTS AND DISCUSSION

Oxygen Investigation

Normalised signal ratios for 28/24 and 16/24 from virgin PGA graphite at different oxygen pressures are shown in Figure 2. The presence of an increased amount of oxygen gave an increased signal intensity at m/z 28, attributed to the formation of CO^- species. As the normalised 28/24 signal is approximately proportional to the normalised 16/24 signal (r^2 0.97) it allows the signal arising from CO^- to be inferred from any given normalised 16/24 signal. The presence of carbon-14 can therefore also be inferred by observing any deviation of the 28/24 ratio to the right of the line. Such deviation implies that there are species present generating a signal at m/z of 28 that are not attributable to CO^-.

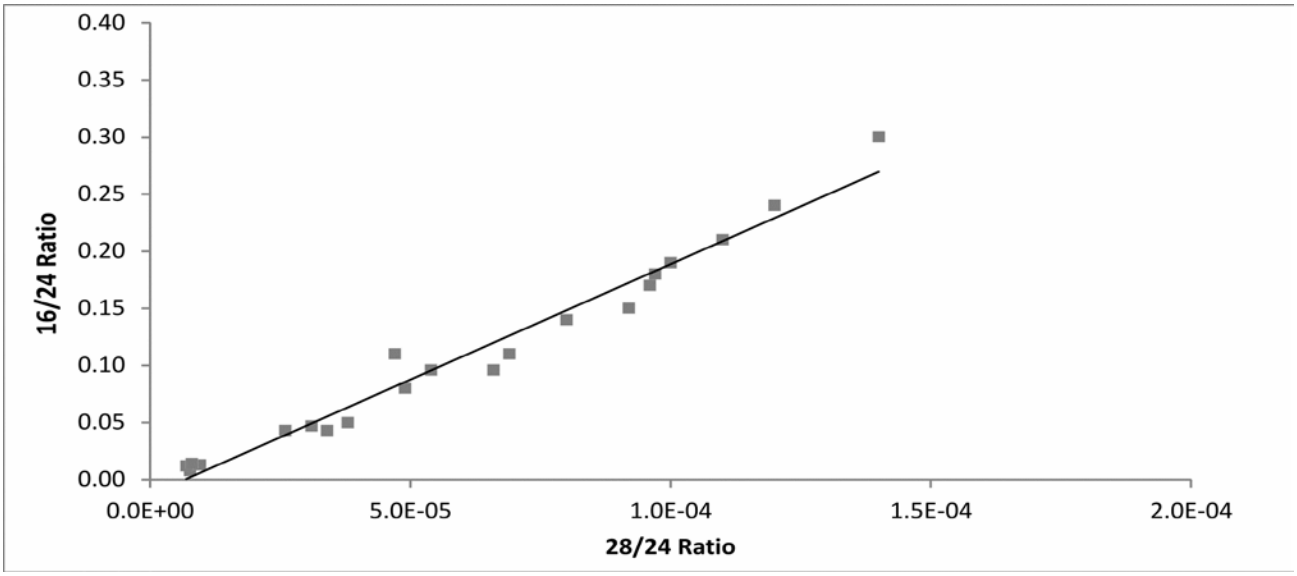

Figure 2: The relationship between the 28/24 and 16/24 normalised signal ratios for virgin PGA exposed incrementally to oxygen during analysis. The m/z = 28 signal is assumed to be from CO^- species generated on the surface.

Irradiated Graphite

The C-14 concentration was determined by calculating the increase, if applicable, between the normalised 28/24 signal and the 28/24 signal attributed to CO^-. As the signal at m/z 24 was expected to be constant the C-14 concentrations results are given in parts per million (ppm). A correction for the contribution of CN was also applied. Standard error of the mean (SE) was calculated for normalised 28/24 and 16/24 signals, these were combined with error values obtained from linear regression analysis performed using Origin data analysis software to give total error values for C-14 concentration.

For ease of visualising results sample surfaces were identified as either from channel wall surfaces or from within the brick. Therefore, for a full trepan set of three samples (six analysed surfaces), one was identified as a channel wall surface and the remaining five combined to give inner brick material thus giving a total of six analyses for each channel wall face and up to thirty for inner brick material.

C-14 concentrations calculated using the method stated above are shown in Table III. The presence of a carbonaceous deposit was determined with Scanning Electron Microscopy (SEM), Figure 3, as these deposits have a markedly different topography to radiolytically oxidised graphite [12]. Analysis of several samples resulted in the normalised 28/24 signal being indistinguishable from the signal arising from CO^-, in such instances the result is stated as below the limits of detection (< LOD).

Comparison of channel wall face samples and inner brick samples highlighted an apparent C-14 enrichment in channel wall face samples between approximately 5 and 55 ppm. C-14 concentrations of inner brick samples were found to be either below the limits of detection, currently estimated as approximately 1-5 ppm, or being unreliable due to having an error value greater than the concentration. There were several exceptions where the C-14 concentration in channel wall face samples was found to not be enriched, notably J01A4 4U, J01A4 7U, M10 7L, N15A4 4U and F16 7L.

TABLE III. C-14 concentrations determined by MS-SIMS for irradiated graphite samples, grey background indicates surfaces with deposit.

Channel	Sample set	Coating Present	C-14 Concentration (ppm)	Error (ppm)
L13B2 7L	Channel Wall Face	Y	12.8	1.5
L13B2 7L	Inner Brick	N	< LOD	< LOD
L13B2 4L	Channel Wall Face	Y	28.8	4.3
L13B2 4L	Inner Brick	N	4.2	1.3
M10 7L	Channel Wall Face	N	< LOD	<LOD
M10 7L	Inner Brick	N	0.7	3.4
M10 4L	Channel Wall Face	Y	55.3	6.7
M10 4L	Inner Brick	N	6.1	4.7
N15A4 8U	Channel Wall Face	Y	19.2	1.1
N15A4 8U	Inner Brick	N	6.9	3.0
N15A4 4U	Channel Wall Face	Y	24.9	8.9
N15A4 4U	Inner Brick	N	9.5	2.0
J15B5 7L	Channel Wall Face	Y	6.6	0.6
J15B5 7L	Inner Brick	N	2.5	1.1
J15B5 4L	Channel Wall Face	Y	28.5	4.9
J15B5 4L	Inner Brick	N	< LOD	< LOD
E19B5 8U	Channel Wall Face	Y	5.4	1.4
E19B5 8U	Inner Brick	N	< LOD	< LOD
E19B5 4U	Channel Wall Face	Y	24.6	0.8
E19B5 4U	Inner Brick	N	0.3	3.1
F16 7L	Channel Wall Face*	Y	22.7	5.5
F16 7L	Channel Wall Face*	N	< LOD	< LOD
F16 7L	Inner Brick	N	< LOD	< LOD
F16 4L	Channel Wall Face	Y	26.1	3.1
F16 4L	Inner Brick	N	16.7	4.0
J01A4 7U	Channel Wall Face	N	< LOD	< LOD
J01A4 7U	Inner Brick	N	< LOD	< LOD
J01A4 4U	Channel Wall Face	N	< LOD	< LOD
J01A4 4U	Inner Brick	N	< LOD	< LOD
Q15C5 11U	Channel Wall Face	Y	5.3	1.8
Q15C5 11U	Inner Brick	N	< LOD	< LOD
Q15C5 7L	Channel Wall Face	Y	13.2	3.9
Q15C5 7L	Inner Brick	N	< LOD	< LOD
Q15C5 6L	Channel Wall Face	N	97.9	23.5
Q15C5 6L	Inner Brick	N	< LOD	< LOD
Q15C5 4L	Inner Brick	N	15.8	6.5
Q15C5 2U	Channel Wall Face	Y	20.8	3.9
Q15C5 2U	Inner Brick	N	4.1	3.4

SEM analysis of the channel wall face samples M10 7L and N15A4 4U showed there was no apparent carbonaceous deposit present, with the reason for this being unknown (the deposit was expected as it was identified on samples from different locations within the same channel, M10 4L and N15A4 8U respectively). F16 7L showed non-uniform coverage with large parts of the surface having no apparent coating and other parts containing the carbonaceous deposit, again for unknown reason. Since there was a clear distinction between areas of the surface with the deposit and without both areas were able to be analysed separately, highlighted by an asterix in Table III, and results show these. J01A4 4U and J01A4 7U were trepanned from the same channel on the outer edge of the reactor core, Figure 4, and their location might be a possible explanation for the lack of carbonaceous deposit on these two samples, since the deposit is believed to be formed from radiolytic polymerisation of carbon monoxide [14] and the neutron flux is reduced at such locations of the reactor core. These samples provide significant evidence that the C-14 enrichment is due to the carbonaceous deposit i.e. samples that were located on the channel wall face but without the deposit do not show C-14 enrichment.

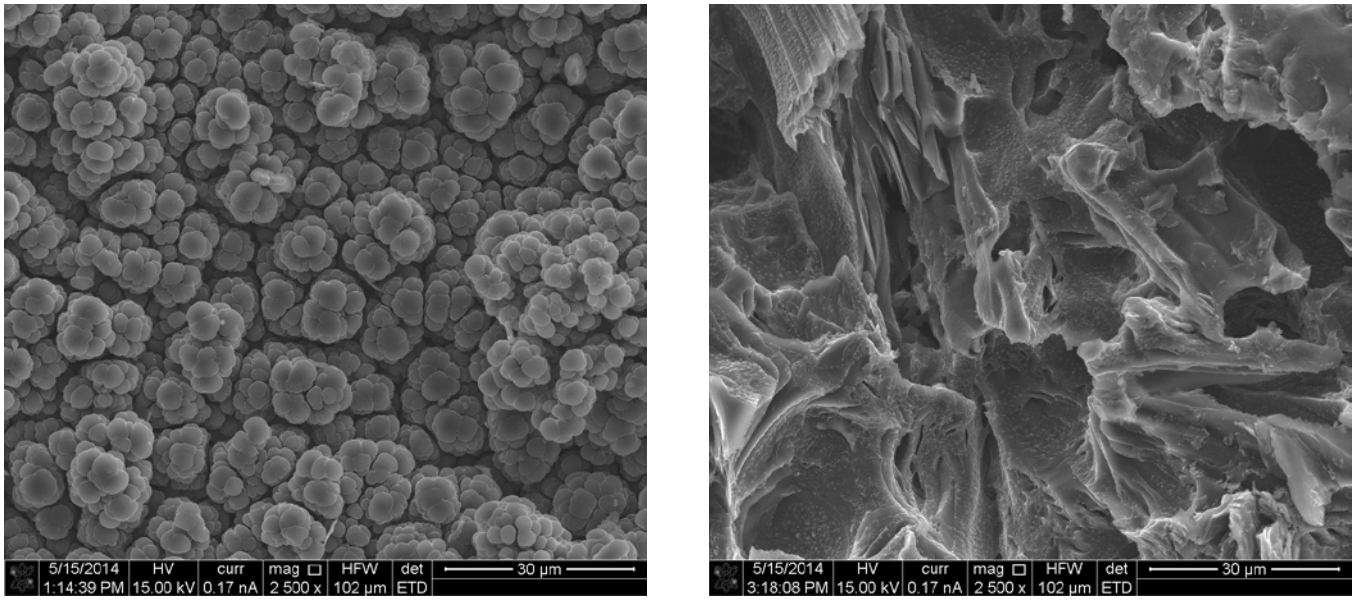

Figure 3: Electron micrographs highlighting the differences in surface topography of irradiated graphite with carbonaceous deposit (left) and without (right), sample M10 4L.

Figure 4 shows the spatial positions within the reactor core, together with the C-14 values measured here, and the expected neutron irradiation dose at each position received from NNL, expressed as the Equivalent DIDO Nickel Dose (EDND). It is seen that the C-14 values measured in the channel wall deposits do not correlate well with the neutron flux values. This also supports the fact that the enrichment is not in the bulk graphite.

C-14 in the deposit is believed to have arisen from transmutation of nitrogen within the material rather than from C-13 because of the relative concentrations and capture cross-sections, and also because there would seem to be no reasonable mechanism for an enrichment of C-13 within the channel wall deposits. It has been suggested [15] that channel wall deposits are thicker at lower positions within the core due to the temperature profile with height, although again this would not readily explain an increase in C-14 concentration. A difference in the dynamics of coating growth with height, leading to incorporation of varying amounts of nitrogen within the coatings following reactor outages and pressure vessel depressurisation may offer an explanation, but further work would be required to provide a definitive answer.

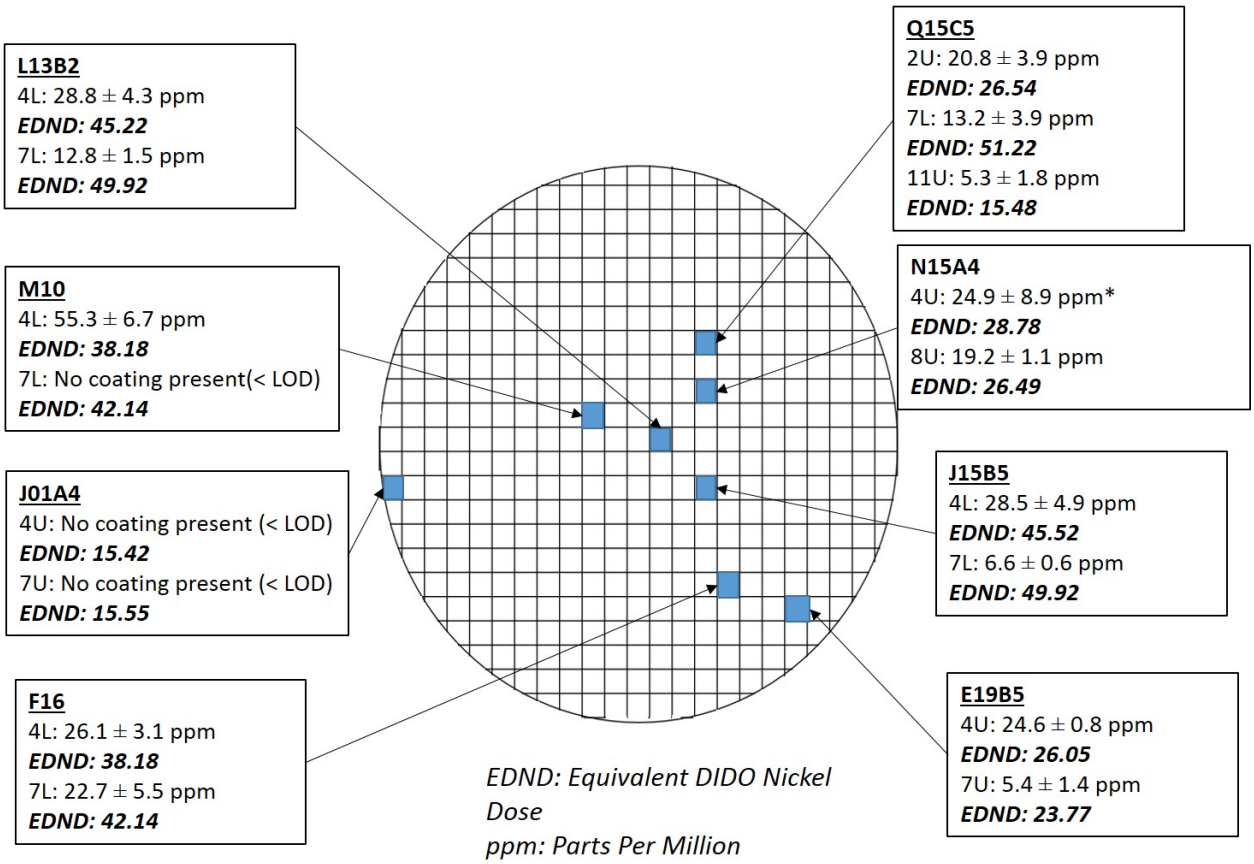

Figure 4: Calculated C-14 concentrations of channel wall face samples highlighting location within the reactor and stated EDND.

CONCLUSION

MS-SIMS has been used to investigate relative C-14 distributions in irradiated graphite from reactor one of Oldbury nuclear power station, a Magnox reactor in the UK. There are limitations in the method, mainly due to limits of detection. However, it has been shown that there is a C-14 enrichment of between approximately 5 and 100 ppm on exposed channel wall surfaces compared to underlying graphite, which is attributed to the carbonaceous deposit formed during the reactor's operating lifetime. Because exposed channel wall surfaces without the deposit did not show C-14 enrichment this builds confidence that the enrichment was due to the deposit and not exposure to the channel wall face itself. Exposed channel wall surfaces at approximately three metres high appear to be significantly more C-14 enriched than those at five metres. However, further work would be required to explain this observation.

REFERENCES

1. Fachinger, J., von Lensa, W., and Podruhzina, T., *Decontamination of nuclear graphite.* Nuclear Engineering and Design, 2008. **238**(11): p. 3086-3091.

2. LaBrier, D. and Dunzik-Gougar, M.L., *Characterization of 14C in neutron irradiated NBG-25 nuclear graphite.* Journal of Nuclear Materials, 2014. **448**(1–3): p. 113-120.
3. Marshall, T.A., Baston, G.M.N., Otlett, R.L., Walker, A.J., and Mather, I.D., *Longer-term release of carbon-14 from irradiated graphite,* 2011, SERCO/TAS/001190/001 Issue 2
4. Mason J. B. and Bradbury, D., *Pyrolysis and Its Potential Use in Nuclear Graphite Disposal. IAEA Technical Committee Meeting on Nuclear Graphite Disposal*, 1999,
5. NDA, *Higher Activity Waste, The Long-term Management of Reactor Core Graphite Waste Credible Options (Gate A)*, 2013, SMS/TS/D1-HAW-6/002/A
6. NDA, *Geological Disposal. Review of baseline assumptions regarding disposal of core graphite in a geological disposal facility.*, 2012, NDA Technical Note no. 16495644.
7. Baston, G., Marshall, T., Otlet, R., Walker, A., Mather, I., and Williams, S., *Rate and speciation of volatile carbon-14 and tritium releases from irradiated graphite.* Mineralogical Magazine, 2012. **76**(8): p. 3293-3302.
8. Yim, M.-S. and Caron, F., *Life cycle and management of carbon-14 from nuclear power generation.* Progress in Nuclear Energy, 2006. **48**(1): p. 2-36.
9. Dunzik-Gougar, M.L. and Smith, T.E., *Removal of carbon-14 from irradiated graphite.* Journal of Nuclear Materials, 2014. **451**(1–3): p. 328-335.
10. White, I.F., Smith, G.M., Saunders, L.J., Kaye, C.J., Martin, T.J., Clarke, G.H., and Wakerley, M.W., *Assessment of Graphite management modes for graphite from reactor decommissioning,* 1984, European Communities Report:EUR 9232 EN.
11. Pickup, I.M., McEnaney, B., and Cooke, R.G., *Fracture processes in graphite and the effects of oxidation.* Carbon, 1986. **24**(5): p. 535-543.
12. Heard, P.J., Payne, L., Wootton, M.R., and Flewitt, P.E.J., *Evaluation of surface deposits on the channel wall of trepanned reactor core graphite samples.* Journal of Nuclear Materials, 2014. **445**(1–3): p. 91-97.
13. Baston, G.M.N., Preston, S., Otlet, R., Walker, J., Clacher, A., Kirkham, M., and Swift, B., *Carbon-14 Release from Oldbury Graphite*, 2014, AMEC/5352/002 Issue 3
14. Wickham, A.J., Sellers, R.M., and Pilkington, N.J., *Graphite Core Stability During "Care and Maintenance" and "Safe Storage"*, 1998, IAEA-TECDOC 1043.
15. Wickham, A.J. and Rahmani, L., *Graphite dust explosibility in decomissioning: A demonstration of minimal risk.*, 2010, IAEA-TECDOC-1647.
16. Heard, P.J., Feeney, K.A., Allen, G.C., and Shewry, P.R., *Determination of the elemental composition of mature wheat grain using a modified secondary ion mass spectrometer (SIMS).* The Plant Journal, 2002. **30**(2): p. 237-245.
17. Ziegler, J.F., Ziegler, M.D., and Biersack, J.P., *SRIM – The stopping and range of ions in matter (2010).* Nuclear Instruments and Methods in Physics Research Section B: Beam Interactions with Materials and Atoms, 2010. **268**(11–12): p. 1818-1823.
18. Payne, L., Heard, P.J, Scott T.B, *Magnetic Sector-Secondary Ion Mass Spectrometry Analysis of Irradiated Graphite Samples from a Magnox Reactor*, in *Poster presented at Implementing Geological Disposal-Technolgy Platform Geodisposal 2014*. 2014: Manchester, UK.

ACKNOWLEDGEMENTS

The authors would like to thank Magnox Ltd. for their support. This work was funded by EPSRC and Radioactive Waste Management in the UK under the GeoWaste contract.